Essential Work of Fracture of Rubber-Modified Polyamide 6 in Impact

EMILIANO LIEVANA, CELINA BERNAL, *and* PATRICIA FRONTINI*

Institute of Materials Science and Technology (INTEMA)
University of Mar del Plata and National Research Council (CONICET)
J.B. Justo 4302, 7600, Mar del Plata, Argentina

In this paper the impact fracture behavior of two commercial, 10% and 25%, rubber-modified polyamide 6 grades is investigated by the Essential Work of Fracture methodology, which implies the testing of a series of samples of different ligament lengths and the determination of the total fracture energy. The study is based on data obtained from specimens made either from thick injected plates or bars. Tests were carried out under Charpy and Izod configuration. Two modes of fracture were displayed by the blends: ductile fracture or mixed mode depending on rubber content, processing conditions and ligament lengths of the samples. When samples displayed completely stable crack propagation behavior and geometric similarity of load-displacements diagrams, an essential work of fracture value w_{le}, independent of specimen thickness and testing configuration, could be extrapolated. Polym. Eng. Sci. 44:1707–1715, 2004.

INTRODUCTION

The growing use of polymeric materials in engineering applications demands new methodologies for assessing the material capability to withstand loads. More specifically, it is well known that thermoplastics, even toughened grades, are relatively susceptible to impact fracture.

The Essential Work of Fracture (EWF), which was first applied for the evaluation of low-rate fracture toughness of very ductile polymers in plane stress (1–5), has been proposed as a useful methodology for evaluating polymer toughness at high rates (6–14) when crack propagation proceeds under stable conditions. The simplicity of the EWF approach is the main reason why the method has become so popular in recent years; for evaluating the fracture toughness of ductile polymers, it is a simpler alternative to *J*-integral analysis. The experimental measurement of the EWF is fairly easy since it simply consists of determining the total fracture energy of several samples differing in the initial ligament length, and the linear regression of these data. In contrast with the *J*-approach, the EWF does not involve the detection of the onset of cracking and the interruption of the test. Previous papers (4, 5, 8) report that the EWF methodology can be applied if the specimen ligament is fully yielded before the onset of crack propagation, and if the plastic zone scales with the square of the ligament length (load-displacement curves self similarity). Under these conditions, the specific EWF is a material constant.

Neat polyamide deformation mechanism is found to be shear yielding (15). The incorporation of an elastomeric secondary phase in polyamides is a well-established means of improving polyamide toughness, especially at high strain rates (11, 16, 17). Rubber toughening in polyamides is achieved by internal rubber particle cavitation, which takes place at the initial steps, relieving the hydrostatic pressure generated in front of the crack tip and hence allowing massive shear yielding to occur in the matrix (15, 16). It is well known that fracture behavior of these multiphase polymers is complex and can be greatly affected by composition, morphology, and testing conditions (16, 18–20).

This paper presents the results of an experimental study of the influence of composition and test configuration on fracture behavior of rubber-modified polyamide 6 assessed by the EWF method. We also aim to give additional insight into the determination of significant high-rate fracture toughness values of these materials, which still appears controversial.

THE ESSENTIAL WORK OF FRACTURE METHODOLOGY

According to Broberg (21), when failure of a test specimen is preceded by extensive yielding and slow crack growth, a toughness parameter called the specific

*To whom correspondence should be addressed.

Published online in Wiley InterScience (www.interscience.wiley.com).
DOI: 10.1002/pen.20171

essential total work of fracture, W_e, can be evaluated. According to the essential work of fracture (EWF) theory (22), the zone in which a crack runs into a material bulk can be divided into two separate regions: a process zone or process plane where the actual crack runs, and a plastic zone, which surrounds the process zone. In the plastic zone, processes related to dissipating mechanisms take place. Consequently, the total work of fracture, W_f, required to fracture a precracked specimen consists of two work components, one referred to as the essential total work of fracture W_e and the other as the non-essential work of fracture, W_p.

The applicability of the EWF methodology relies on the following conditions being satisfied: 1) the ligament should fully yield prior to fracture initiation; 2) the essential fracture work W_e inside the inner fracture process zone should be proportional to the ligament length, l; and 3) the plastic work W_p in the outer process zone should be proportional to the square of the ligament length, l^2, irrespective of the shape of the plastic zone. Thus, the total work of fracture W_f can be written as:

$$W_f = W_e + W_p \tag{1}$$

Divided by the ligament area, lB, (where B is the specimen thickness), *Eq 1* becomes (22, 23):

$$w_f = w_e + \beta.w_p.l \tag{2}$$

in which w_f is the specific fracture work, w_e is the specific essential work of fracture, w_p is the specific plastic work and β is the geometrical shape factor for the outer plastic zone. When plane stress conditions prevail for all ligament lengths, it is further assumed that w_e is constant (2). Hence, it can be seen from *Eq 2* that a linear relationship exists between w_f and l as long as the product $\beta\, w_p$ remains constant.

When the ligament l is small, situation that is usually given by the condition,

$$l \leq (3 - 5).B \tag{3}$$

the plastic constraint increases, which makes the stress condition in the ligament region become one of plane-stress/plane-strain rather than pure plane stress (3, 23, 24). For conditions other than plane stress, w_e is a function not only of l, but also of the specimen thickness B, i.e., $w_e = w_e(l, B)$, while $\beta.w_p$ does not depend on l. Under these circumstances a plane-strain EWF w_{le} can also be obtained from the extrapolation to zero ligament length (23, 24) of the energy data within the plane-stress/plane strain transition region (2, 23–25).

The plane strain regime is reached when the specimen thickness B verifies the well-known condition devised for the critical J-Integral measurements,

$$B > 25.w_{le}/\sigma_y \tag{4}$$

where σ_y is the yield stress of the material, and w_{le} is the plane strain specific essential work of fracture, which is suggested to be a material constant independent of sample geometry (3, 26).

EXPERIMENTAL

Studies were performed on two commercial grades of rubber-modified polyamide 6 resin having 10% and 25% rubber content, respectively. Neat polyamide 6 was also characterized as a reference. Static tensile properties were determined using an Instron 4467 dynamometer at 5 mm/min on Type IV ASTM D638-93 injection-molded specimens of 3-mm thickness (the tensile strength (σ_y) was 59.8 MPa, 38.8 MPa and 18.9 MPa for polyamide 6, 10% and 25% rubber-modified polyamide 6 respectively).

The three grades were provided in the form of injection-molded plaques of $6 \times 120 \times 150$ mm^3 from which single-edged notched bend (SE(B)) specimens of $6 \times 12 \times 60$ mm^3 were obtained in order to establish the effect of rubber content (*Fig. 1a*). Injection-molded bars of 25% rubber-modified polyamide grade were also available. Three-point-bend specimens were prepared from 10×15 mm^2 cross section bars by directly cutting the bars perpendicularly to the injection direction (*Fig. 1b*). Cantilever specimens were obtained from 15×15 mm^2 cross section bars by first cutting the bars perpendicularly to the injection direction and then machining the four resulting perpendicular faces in order to reach final dimensions 12.7×12.7 mm^2 (*Fig. 1c*). Sharp notches of different depths were introduced in all the specimens as described elsewhere (27). Final ligament lengths ranged from 2 mm to 11 mm. Samples were dried in a vacuum oven at 80°C for 16 h before testing.

Impact tests were carried out in both three-point-bend (Charpy) and cantilever (Izod) configurations using an instrumented Fractovis (CEAST) falling weight, at an impact velocity of 2 m/s at 23°C. Aiming to reduce dynamic effects, mechanical damping consisting of a silicon grease layer of 0.2-mm thickness was used in all the tests by following the ESIS Protocol recommendations (28). The amount of energy absorbed in all tests was calculated by computational integration of the load-displacement plots. In every case, energy corrections for machine compliance and specimen indentation were estimated from separate tests performed on un-notched specimens as described in Ref. 29.

To calculate the essential work of fracture, the total energy to failure per unit area of the ligament was plotted versus ligament length. From the least-squares linear regression of the data (*Eq 2*), values of w_{le} and w_p were determined as the y-intercepts and the slopes of the line, respectively. Note that in the range of thickness used, the ligament lengths were much shorter than *5B*, and consequently the data obtained are expected to be in pure plane strain regime (23°C) (30).

The morphology of the two blends was investigated by performing cryo-fracture on the specimens and then etching them in boiling xylene to be observed by SEM.

EXPERIMENTAL RESULTS

Effect of Rubber Content

Figure 2 shows SEM fractographs of xylene-etched surfaces of the cryo-fractured specimens of the two

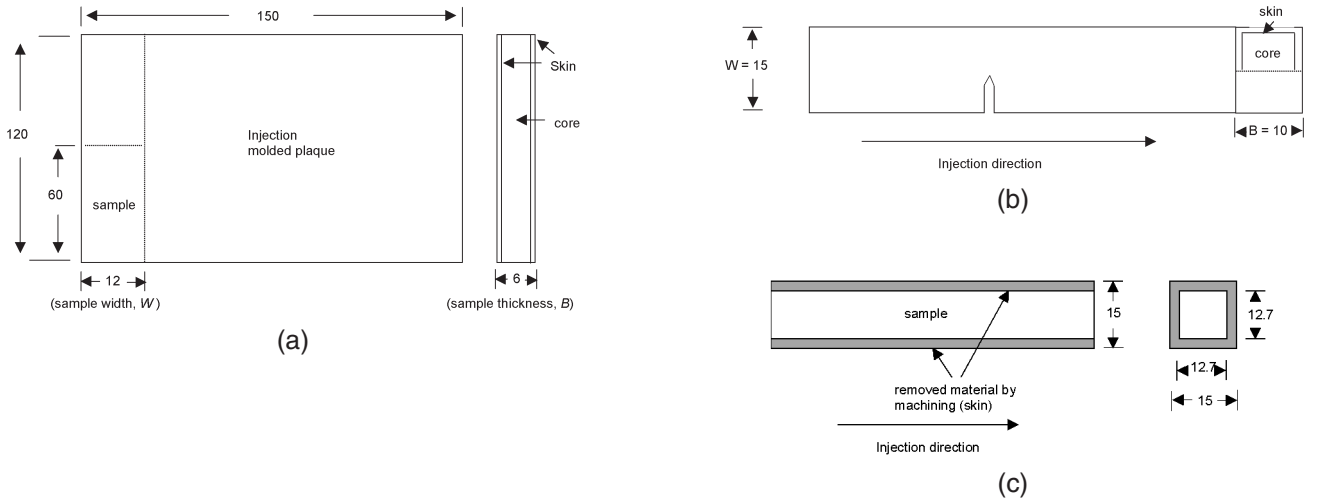

Fig. 1. Schematic of sample geometries. a) Samples obtained from injection-molded plaques. b) Samples obtained from injection-molded bars without machining. c) Samples obtained from injection-molded bars with machining.

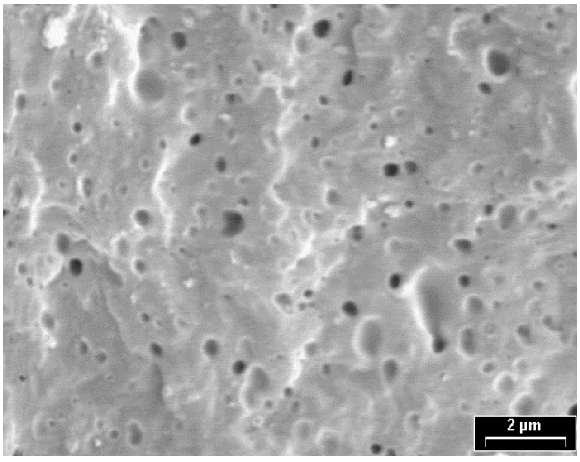

(a)

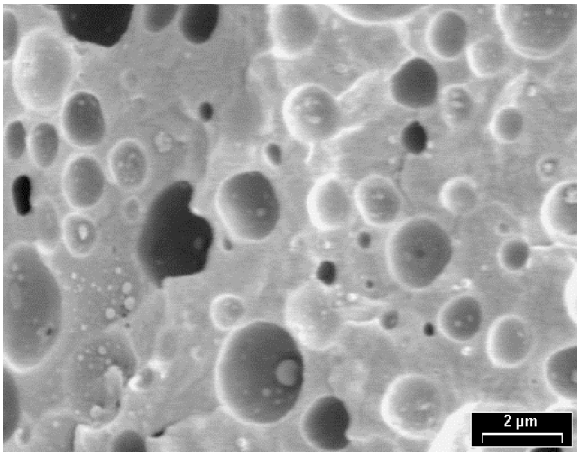

(b)

Fig. 2. Cryogenic fractured and etched (in boiling xylene) surface of rubber toughened polyamide 6. a) 10% rubber-modified polyamide 6. b) 25% rubber-modified polyamide 6.

blends. Rubber appears to be well dispersed in the nylon matrix for both compositions even if a finer dispersed rubber morphology can be appreciated in the 10% rubber blend (*Fig. 2a*). No differences in rubber morphology across the thickness were revealed by SEM analysis.

Load-displacement records and fracture surface analyses (*Fig. 3*) revealed that neat resin behaved brittlely under high strain rate, consistent with the behavior previously reported for polyamide 6 (18). Upon reaching the maximum load, unstable crack propagation with a precipitous load drop to zero was observed. No signs of shear yielding (shear lips) were displayed by fracture surfaces. The brittle nature of the failure is thought to be mainly caused by the high speed of the impact test, since in slow-speed notch-bending tests, polyamide 6 samples exhibit ductile behavior related to shear banding formation (31). Accordingly, the fracture toughness of the neat polyamide 6 was assessed following the Energy Release Rate approach (29) (*Fig. 4*). The energy absorbed up to the energy peak was used to calculate the initiation fracture energy G_{IC} by:

$$G_c = \frac{U}{\phi \cdot B \cdot W} \tag{5}$$

where ϕ is the energy calibration factor depending upon support span to width ratio (S/W) and crack length to width ratio (a/W) of a given specimen configuration.

A completely different pattern was found in the case of rubber-modified polyamide specimens (*Fig. 5*). In 10% rubber samples, the mode of fracture was dependent on the ligament length, as judged from the load-displacement response (*Fig. 5a*). Load-displacement patterns revealed that in samples having ligament lengths shorter than a critical value (9 mm), crack propagation was completely stable. On the other hand, unstable linear-elastic behavior occurred in samples

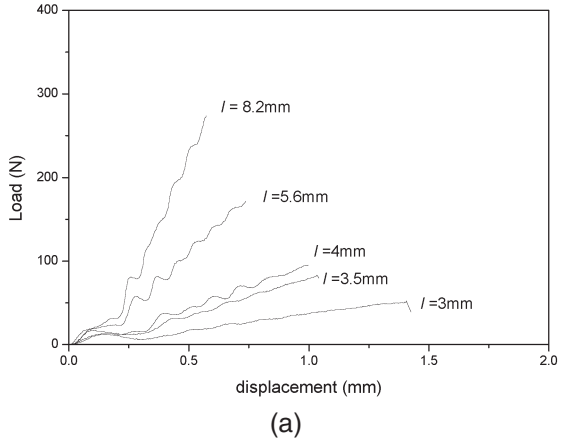

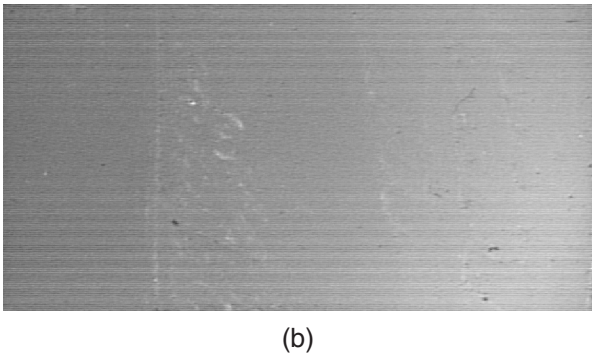

Fig. 3. a) Load-displacement records for polyamide 6 specimens cut from injection molded plaques tested in three-point-bend configuration. b) Corresponding fracture surface.

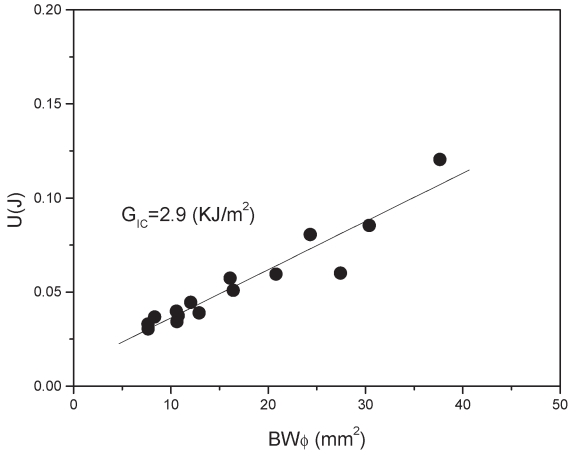

Fig. 4. Fracture energy versus BWϕ for neat polyamide 6.

with longer ligament lengths. In brief, our results present a transition from ductile to brittle fracture with ligament length.

The ductile-to-brittle transition with ligament length this blend underwent was also reflected in the EWF plot (*Fig. 5b*). The specimens that failed in a ductile

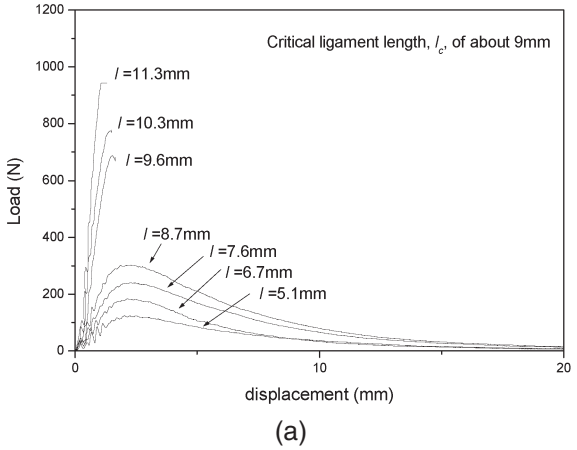

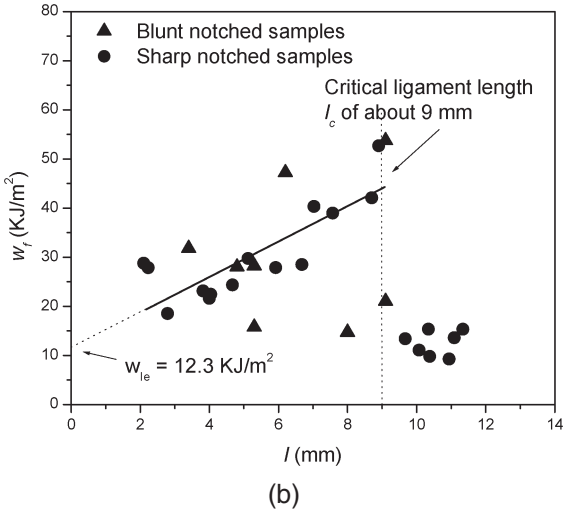

Fig. 5. a) Load-displacement records for 10% rubber-modified polyamide 6 samples showing stable crack propagation for specimens with l < lc (lc is the critical ligament length, which is about 9 mm) and unstable linear-elastic behavior for specimens with l > lc. b) Specific fracture energy versus ligament length for 10% rubber-modified polyamide samples showing an increasing trend of these values for samples with l < lc and lower values for samples with l > lc.

manner displayed high specific fracture energy values, while specimens that failed in brittle manner displayed very low specific fracture energy values. In the range of ligament lengths where self-similarity of the load-displacement curves (stable propagation) was verified, data points could be satisfactorily analyzed by the EWF model. Ductile-brittle transitions dependent on loading rate and specimen geometry have been previously observed in fracture behavior studies of ductile polymers through the EWF method (32).

Above the critical ligament length data were analyzed by the Critical Energy Release Rate parameter, leading to a G_{IC} average value of 15.6 KJ/m^2. In this way the entire range of behavior was quantified. Values of w_e and G_{IC} were not very different, indicating that the

larger specific fractures energies displayed by ductile samples stem from the work dissipated in the plastic zone during stable crack growth.

The difference between brittle and ductile fracture also appears clear from the fracture surface features (*Fig. 6*). When the specimen broke in the brittle way, stress-whitening could only be observed at a distance of 1.5 mm from the crack initiation (*Fig. 6a*). Similar results were reported in the literature (11, 18). Besides, ductile samples exhibited stress-whitening through the whole fracture surface, with clear lateral constriction (*Fig. 6b*).

All 25% rubber-modified polyamide specimens displayed stable crack propagation, irrespective of the ligament length used (*Fig. 7a*). However, self-similarity of load-displacement curves was lost for specimens with relatively long ligaments. Consistently, beyond a certain critical ligament length, EWF plots showed a decreasing trend with ligament lengths (*Fig. 7b*). Observation of EWF plots reveals that this phenomenon differs from the ductile-brittle transition observed in 10% blends (*Fig. 5b*).

The detailed inspection of fracture surfaces (see *Fig. 8*) of this particular composition revealed an anisotropic layer-like structure induced by the injection molding process with distinct properties across the thickness (*Fig. 8*). All samples exhibited a stress-whitened central zone surrounded by a brittle skin layer.

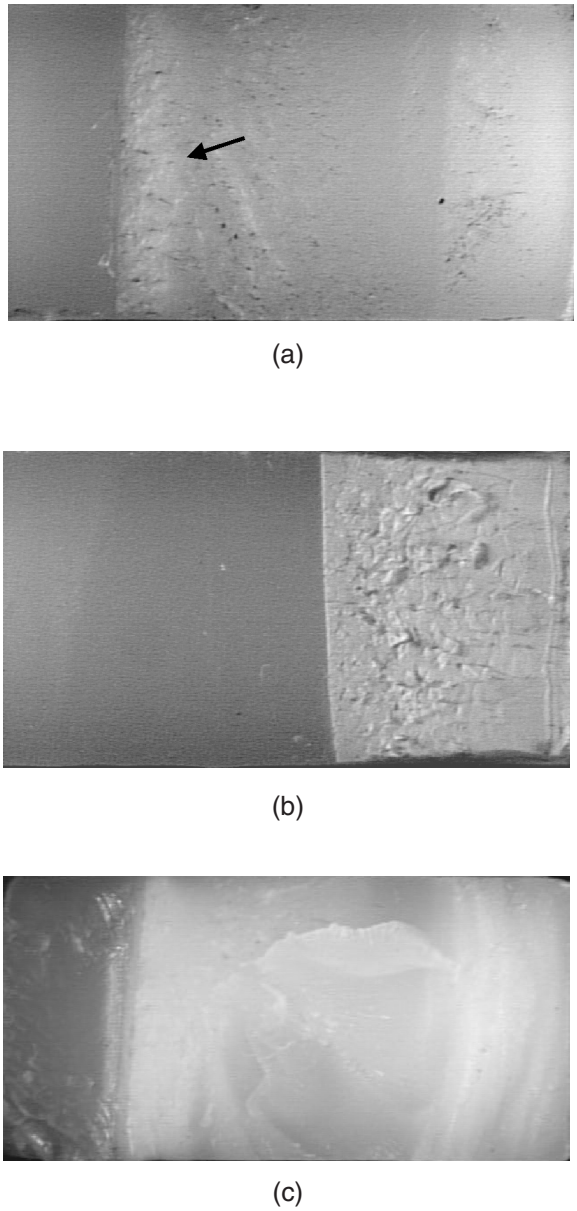

Fig. 6. Fracture surfaces of 10% rubber-modified polyamide 6 samples (the crack propagated from left to right). a) Brittle sharp-notched sample with stress-whitening only at a distance of a few millimeters from the notch tip (arrow). b) Ductile sharp-notched sample exhibiting stress-whitening through the whole fracture surface as well as clear lateral constriction. c) Blunt-notched sample exhibiting less stress-whitening than ductile sharp-notched sample.

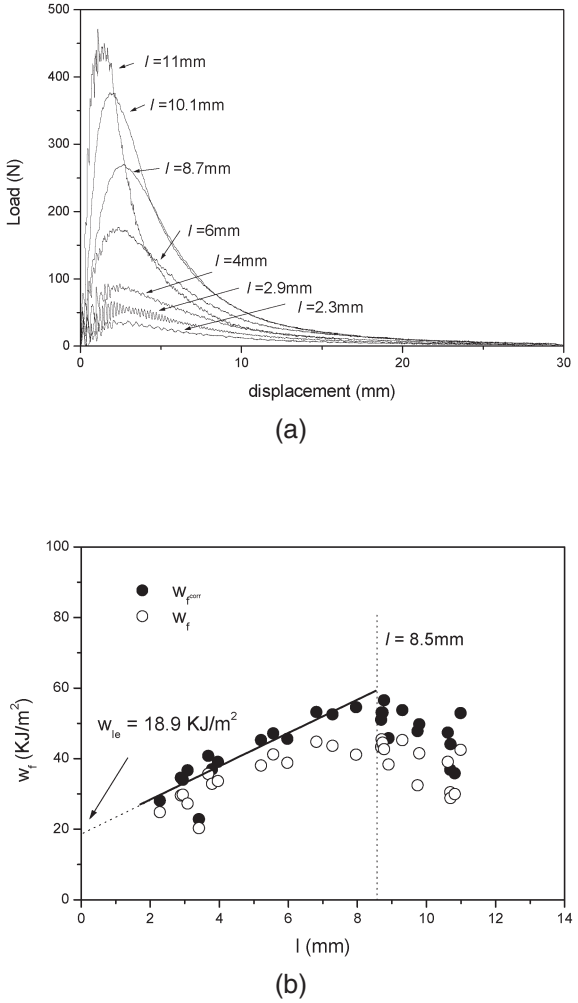

Fig. 7. a) Load-displacement records for 25% rubber-modified polyamide 6 samples. b) Specific fracture energy versus ligament length for 25% rubber-modified polyamide samples indicating the ligament length equal to 8.5 mm from which data points could not be regressioned by the EWF model.

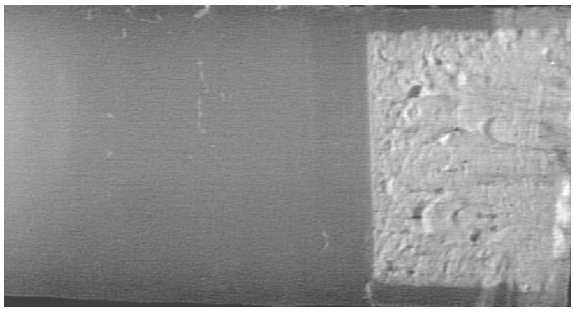

(a)

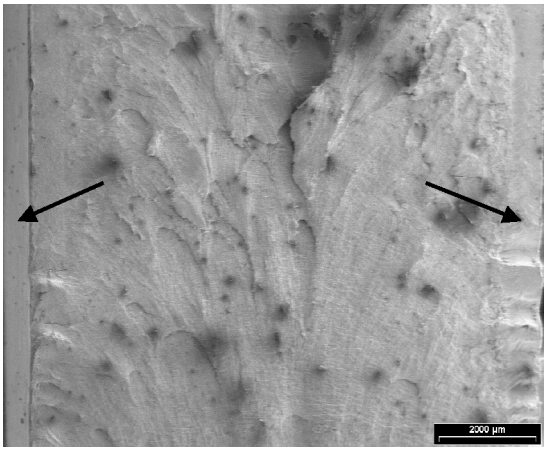

(b)

Fig. 8. Fracture surfaces of 25% rubber-modified polyamide showing processing-induced skin-core morphology (the crack propagated from the left to the right). a) Optical micrograph; b) SEM micrograph (arrows indicate the skin layers).

A sharp boundary between the skin and core characterizes the skin-core structure, this boundary being able to promote premature fracture (17, 33–35). It has been already reported that the essential work of fracture parameters of injection molding nylon 6 samples can be affected by the surface layer and morphology gradient exhibited by these samples (32).

Following the proposal of Karger-Kocsis (36), we corrected the EWF by subtracting the brittle area from the total fracture plane assuming that the brittle part of the fracture surface has very little contribution to the total work of fracture.

$$w_f^{corr} = W_f / A^{corr} \quad (5)$$

where A^{corr} is the corrected area equal to $l^{corr}.B$.

The effective ligament length l^{corr} is calculated as:

$$l_{corr} = l - l_B \quad (6)$$

where l is the initial ligament length and l_B is the length of the brittlely fractured ligament path.

A clearly linear reduction of the fracture energy with increasing ligament length could not be confirmed (*Fig. 7b*). Only in the small range of ligament lengths (where self-similarity of the load-displacement curves was verified) could data points be regressioned by the EWF model (*Fig. 7b*).

It has been stated that for plane strain linear elastic behavior the critical J-Integral value J_C becomes identical to the critical strain energy release rate, G_{IC} (37). Using geometric similarity arguments between J and w_f, Mai and Cotterell (38) demonstrated that w_e is equivalent to J_C. Therefore the two parameters obtained (G_{IC} and w_e) can be compared. An increasing trend of dynamic fracture toughness values with rubber content was found within the range assessed (*Figs. 4*, *5b* and *7b*).

Effect of Test Configuration

The 25% rubber-modified polyamide samples prepared from injection-molded bars displayed completely stable crack propagation, as observed in the load-displacement curves reported in *Figs. 9a* and *9b*, irrespective of the test configuration, Charpy or Izod. Since a smaller relative area was affected by the processing-induced skin-core morphology, no detrimental effects were detected in this type of specimen. Each set of

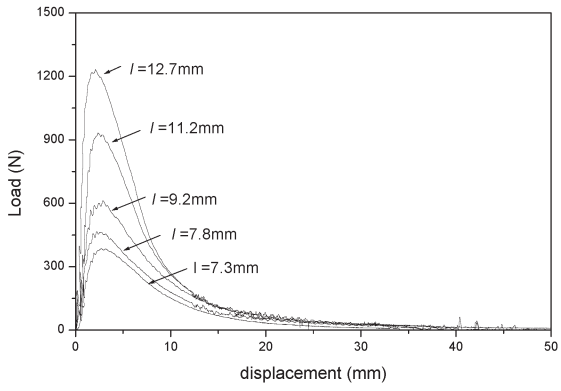

(a)

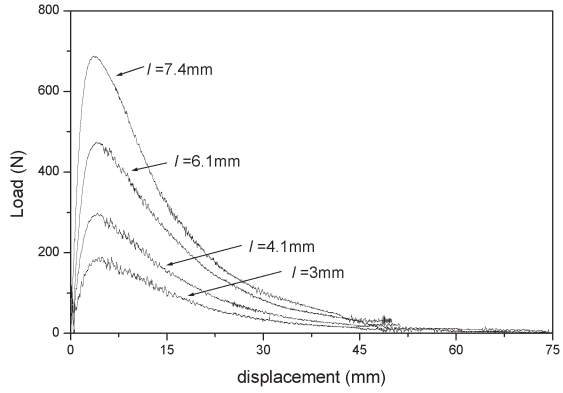

(b)

Fig. 9. Load-displacement records for 25% rubber-modified polyamide 6 samples obtained from injection-molded bars. a) Samples tested in three-point-bend configuration; b) samples tested in Izod configuration.

curves is self-similar, and hence the geometric similarity prerequisite of the EWF method was verified in every case.

Figure 10 compares cantilever with three-point-bend EWF results. While the specific non-essential work of fracture (βw_p) is dependent on the testing configuration due to the change in the plastic zone shape factor with change in geometry (30), no significant differences in the specific essential work of fracture for the two configurations and the two specimen thicknesses assayed were detected. This result confirms that the *a priori* expected plane strain conditions were met.

DUCTILE-TO-BRITTLE TRANSITION

The phenomenon of ductile-brittle fracture transition has been observed in many engineering materials (39–41). Changes in test temperature and loading rate may cause a ductile-brittle fracture transition that can be explained in terms of the elevated yield stress of the material. Another well-known cause for a ductile-brittle transition is associated with the change of stress-strain state ahead of the crack tip due to the transition from plane stress to plain strain fracture induced by the increase in thickness plate.

A ductile-to-brittle transition with ligament length analogous to the one exhibited by the 10% rubber-modified polyamide 6 (*Fig. 5b*) was reported in a rubber-toughened polyamide 6 and their blends with acrylonitrile-butadiene-styrene terpolymer (11–13). This decrease in the specific fracture energies at large ligament lengths constitutes an anomalous behavior. Slip-line field and finite-element analysis (42–45) showed that the hydrostatic stresses are generally larger for deeper cracks ($a/W > 0.2$–0.3) and that the normalized crack depth (a/W) has a significant effect on the constraint level ahead of the crack tip. Consequently a decrease in crack length may cause a transition of fracture mechanisms from ductile tearing to brittle cleavage (46) in opposition to the ductile-to-brittle transition phenomenon with ligament length suffered by 10% rubber-modified polyamide 6 (see **Effect of Rubber Content** section). The first approach we tried to interpret the changes in fracture mode with ligament length was the critical stress model for cleavage fracture, since it was previously suggested in a similar case (12). It proposes that unstable cleavage fracture occurs when the local tensile stress (σ_{yy}) ahead of a stress concentrator exceeds a critical stress (σ_f). If ductile failure occurs by tensile yielding at a stress of σ_y, the failure stress can be calculated from the tensile stress at the position of the crack tip based on the so-called "net section" argument:

$$\sigma_f = \sigma_y.[(W - a)/W]^2 \tag{7}$$

If brittle failure occurs, linear elastic fracture mechanics predicts that under plane-strain conditions failure occurs at:

$$\sigma_f = K_{IC}/(Y.\sqrt{a}) \tag{8}$$

where K_{IC} is the critical stress intensity factor and Y is the geometrical factor for the geometry used (39). In order to check the proposed model, the failure stress, calculated from the peak load of the load-displacement data, should be plotted against crack length (a/W) and fitted according to their behavior. Ductile mode failed data were fitted by using the yield stress model while brittle mode failed data were fitted by using K_{IC} model (11–13). If data follow the so-called "Failure Stresses Model" at short ligaments or long cracks, the failure stress by ductile yielding should be smaller than the failure stress by brittle crack propagation and an intersection of the corresponding fittings should exist at the transition ligament length. However, the two curves did not intersect at all, and the failure stresses obtained by extrapolating the K_{IC} model at short ligaments (long cracks) were clearly higher than the failure stresses corresponding to ductile yielding (*Fig. 11*). Consequently, the model was laid aside.

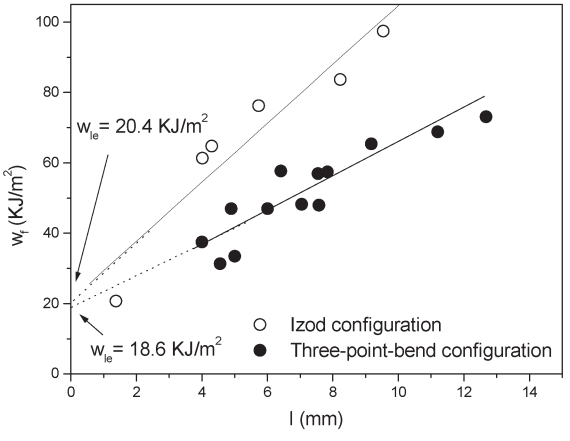

Fig. 10. Specific fracture energy versus ligament length for 25% rubber-modified polyamide samples tested in cantilever and three-point-bend configuration.

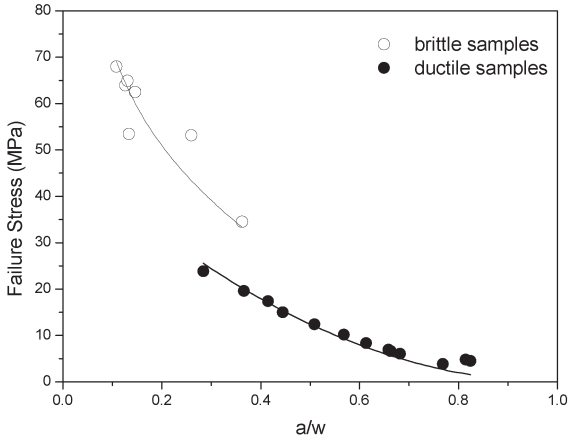

Fig. 11. Failure stress versus normalized crack length (a/W) for 10% rubber-modified polyamide samples.

The reported behavior resembles the sudden instability that occurred in fracture testing of some ductile polymers for large gauche-length samples or blunt-notched specimens (46–48). The tearing modulus approach (49) postulates that unstable cracking occurs if the applied tearing modulus (T_a) exceeds the material tearing modulus (T_m). T_a is the system's driving force for crack growth that depends on the stiffness of the test system being used, while T_m is the material's resistance to crack growth that may be assumed to be a material property (50). Since the crack growth driving force is the release rate of stored elastic energy, large (45), blunt-notched (46), or long ligament samples (51) have higher capability of storing elastic energy. Even if we are not able to quantitatively determine the applied tearing modulus under the experimental conditions used here (39, 50), a qualitative interpretation of the phenomenon based on the tearing modulus concept will be made in what follows.

Extra experiments were carried out using similar-dimension blunt-notched specimens (see triangles in *Fig. 5b*), which, unless they have lower constraint at the notch tip, appear more prone to produce instability. It can be said that T_a increases with increasing notch tip radius. Therefore, a larger notch tip radius is more prone to produce instability if the material's resistance to crack growth T_m is not significantly affected by the notch sharpness (46). Consistent with the tearing modulus model, at ligament length levels in which sharp notched specimens still show completely ductile failure, instability in the specimens with blunt notches occurs just after crack initiation, as indicated by the steep fall in the load-displacement curves for blunt notched samples (*Fig. 12*). Because of the higher stress concentration at the tip of the sharp notch, crack initiation occurs at a lower load level (*Fig. 12*). Hence, less elastic energy is stored at that point, and the driving force results are lower for the sample with the sharp notch.

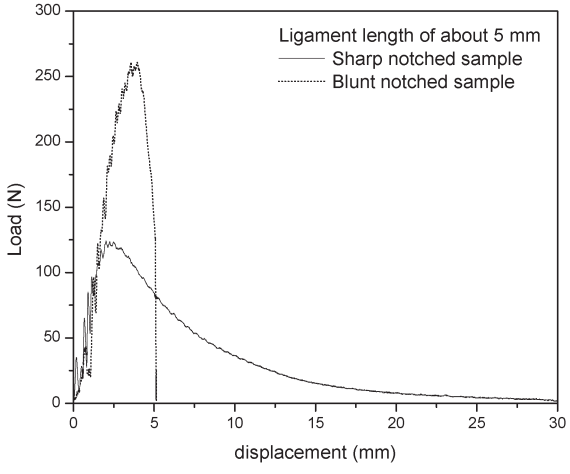

Fig. 12. Load-displacement records for 10% rubber-modified polyamide blunt-notched and sharp-notched samples.

Fracture surface analysis also revealed less stress-whitening for blunt-notched samples (*Fig. 6c*).

Similarly, the sudden instability observed for 10% rubber-modified polyamide can be attributed as well to the higher amount of elastic energy stored in samples with long ligament lengths.

CONCLUSIONS

The specific fracture work concept has been applied to characterize the fracture behavior of rubber-modified polyamide samples. The following conclusions can be drawn from this work.

Changes in fracture behavior associated with the ligament length of each individual specimen were found. Ten-percent (10%) rubber-modified polyamide went through a transition in the fracture mode, which was clearly reflected in the appearance of the fracture surface, since the stable propagation mode led to stress-whitened fracture surfaces. Samples with long ligament lengths exhibited brittle behavior with low energy values, whereas samples with short ligament lengths exhibited ductile failure with high energy values. Unfortunately, a simple model available in literature based on competition between ductile and brittle fracture (11) did not fit our results. This dual mode of fracture could be attributed, at least qualitatively, to the larger elastic energy stored in samples with long ligament lengths, in agreement with the tearing modulus analysis.

For 25% rubber-modified polyamide samples, a processing-induced skin layer that behaves brittlely was observed in 6-mm-thick samples. Over a certain critical ligament length, the processing-induced anisotropic layer-like structure dramatically affected overall fracture behavior, lowering specific fracture energies and hence confirming the influence of the brittle skin layers on the fracture behavior reported for nylon 6 (32). This negative effect was observed only for long ligament samples.

Whenever geometric similarity was verified, the specific essential fracture work concept allowed determination of the fracture toughness of materials. This requirement appears as a very important precondition for the EWF methodology to be effective. The ductile-brittle transition dependent on ligament length and also the influence of the brittle skin layers on fracture behavior impose a severe drawback to the method.

Within the ligament range in which methodology requirements were met, independency of the w_{le} value of sample thickness and test configuration (Izod and Charpy) was proved for 25% rubber-modified polyamide.

From the results obtained here, it appears that some aspects of the EWF still appear controversial.

REFERENCES

1. H. Chan and J. G. Williams, *Polymer*, **35**, 1666 (1994).
2. C. A. Paton and S. Hashemi, *J. Mater. Sci.*, **27**, 2279 (1992).
3. Y-W. Mai and P. Powell, *J. Polym. Sci., Part B: Polym. Phys.*, **29**, 785 (1991).
4. S. Hashemi, *J. Mater. Sci.*, **28**, 6178 (1993).

5. S. Hashemi and D. O'Brien, *J. Mater. Sci.*, **28**, 3977 (1993).
6. F. Martinatti and T. Ricco, *Proceedings of Impact and Dynamic Fracture of Polymers and Composites*, ESIS 19, J. G. Williams and A. Pavan (1995).
7. L. Fasce, V. Pettarín, C. Bernal, and P. Frontini, *J. Appl. Polym. Sci.*, **74**, 2681 (1999).
8. J. M. Hodgkinson, K. H. L. Chow, and J. G. Williams, *Proc. 8th International Conference on Deformation Yield and Fracture of Polymers*, Cambridge (1991).
9. A. Pegoretti, A. Marchi, and T. Ricco, *Polym. Eng. Sci.*, **37**, 1045 (1997).
10. O. F. Yap, Y-W Mai, and B. J. Cotterell, *J. Mater. Sci.*, **18**, 657 (1983).
11. O. Okada, H. Keskkula, and D. Paul, *Polymer*, **41**, 8061 (2000).
12. R. Kudva, H. Keskkula, and D. Paul, *Polymer*, **41**, 335 (2000).
13. T. Pressly, H. Keskkula, and D. Paul, *Polymer*, **42**, 3043 (2001).
14. O. Santana, M. L. Maspoch, and A. B. Martínez, *Polymer Bulletin*, **39**, 511 (1997).
15. R. J. Gaymans, *Toughened Polyamides in Rubber Toughened Engineering Plastics*, A. A. Collyer, ed., Chapman and Hall (1994).
16. R. Borggreve, R. Gaymans, and H. Eichenwal, *Polymer*, **30**, 78 (1989).
17. E. A. Flexman, *Toughened Plastic I. Science and Engineering*, Ch. 4, C. K. Riew and A. Kinloch, eds., American Chemical Society (1993).
18. R. Borggreve, R. Gaymans, J. F. Schuijer, and I. Housz, *Polymer*, **28**, 1489 (1987).
19. R. Borggreve and R. J. Gaymans, *Polymer*, **30**, 63 (1989).
20. R. Borggreve, R. J. Gaymans, and J. Schuijer, *Polymer*, **30**, 71 (1989).
21. K. B. Broberg, *Int. J. Fract.*, **4**, 11 (1968).
22. Y-W. Mai, S-C. Wong, and X-H. Chen, *Application of Fracture Mechanics for Characterization of Toughness of Polymer Blends. Polymer Blends, Vol. 2: Performance*, D. R. Paul and C. B. Bucknall, eds., John Wiley & Sons, Inc. (2000).
23. Y-W. Mai and B. Cotterell, *Int. J. Fract.*, **32**, 105 (1986).
24. A. S. Saleemi and J. A. Nairn, *Polym. Eng. Sci.*, **30**, 211 (1990).
25. J. S. Wu and Y-W. Mai, *Polym. Eng. Sci.*, **36**, 2275 (1996).
26. Y-W. Mai, B. Cotterell, R. Horlyck, and G. Vigna, *Polym. Eng. Sci.*, **27**, 804 (1987).
27. C. Bernal, A. Cassanelli, and P. Frontini, *Polymer Testing*, **14**, 85 (1995).
28. A. Pavan and J. G. Williams, ASTM STP 1369, J. S. Peraro, ed., *American Society for Testing and Materials*, Conshohocken, Pa. (1999).
29. ISO/DIS 17281 Standard, *Plastics—Determination of Fracture Toughness* (G_{IC} *and* K_{IC}) *Standard for Determining for Plastics at Moderately High Loading Rates* (*1 m/s*). Ausgabe (2001−03).
30. S. Hashemi, *Polym. Eng. Sci.*, **40**, 798 (2000).
31. S. Hashemi and J. G. Williams, *J. Mat. Sci.*, **26**, 621 (1991).
32. R. S. Yamakawa, C. A. Razzino, C. A. Correa, and E. Hage Jr., *Polymer Testing*, **23**, 195 (2004).
33. J. Karger-Kocsis, "Microstructural and Molecular Dependence of the Work of Fracture Parameters in Semicrystalline and Amorphous Polymer Systems," in *Fracture of Polymers, Composites and Adhesives*, ESIS Publ. Vol. 27, J. G. Williams and A. Pavan, Elsevier Sci., Oxford (2000).
34. K. Friedrich and J. Karger-Kocsis, *Solid State Behavior of Linear Polyesters and Polyamides*, Chapter 5, J. M. Schultz and S. Fakirov, eds., New Jersey (1990).
35. J. Karger-Kocsis, D. Mouzakis, G. Ehrenstein, and J. Varga, *J. Appl. Polym. Sci.*, **73**, 1205 (1999).
36. D. Mouzakis and J. Karger-Kocsis, *Polymer Bulletin*, **42**, 473 (1999).
37. S. F. Xavier, J. M. Schultz, and K. Friedrich, *J. Mater. Sci.*, **25**, 2411 (1990).
38. Y-W. Mai and B. Cotterell, *Int. J. Fract.*, **32**, 105 (1986).
39. T. L. Anderson, *Fracture Mechanics: Fundamentals and Applications*, CRC Press, Texas (1995).
40. A. J. Kinloch and R. J. Young, *Fracture Behaviour of Polymers*, Applied Science Publishers Ltd., London (1983).
41. S. J. Wu, *J. Appl. Polym. Sci.*, **35**, 549 (1988).
42. B. Matsoukas, B. Cotterell, and Y-W. Mai, *J. Mech. Phys. Solids*, **34**, 499 (1986).
43. C. Yan and Y-W. Mai, Int. *J. Pressure Vessels and Piping*, **77**, 313 (2000).
44. R. H. Dodds, T. L. Anderson, and M. T. Kirk, *Int. J. of Fracture*, **48**, 1 (1991).
45. J. G. Williams, *Fracture Mechanics of Polymers*, Ellis Horwood, England (1984).
46. M. E. J. Dekkers and S. Y. Hobbs, *Polym. Eng. Sci.*, **27**, 1164 (1987).
47. E. Ching, R. K. Y. Li, and Y-W. Mai, *Polym. Eng. Sci.*, **40**, 310 (2000).
48. S-X. Wu, Y-W. Mai, B. Cotterell, and L. C. Viet, *Acta Metall. Mater.*, **39**, 2527 (1991).
49. P. C. Paris, H. Tada, A. Zahoor, and H. Ernst, *Elastic-Plastic Fracture: First Symposium*, ASTM STP 668, 5 (1979).
50. I. Narisawa and T. Takemori, *Polym. Eng. Sci.*, **28**, 1462 (1988).
51. V. Kumar, M. D. German, and C. F. Shih, EPRI Report NP-1931 (1981).